

The small separation of the satellites from the main line implies an equally small difference-potential well depth. The internuclear separation corresponding to this well can be determined from the satellite intensity, and is approximately 25 Å. This is in a region in which the ground-state interaction is not significant.¹⁶ Thus only details of the excited-state potential are responsible for the observed spectrum, and the excited-state must have a well depth of about 10 cm⁻¹. Such a well depth cannot involve significant numbers of bound states at the temperature of the absorption cell.¹⁷ The growth of the satellites can then be used to show that they originate as multiple-perturber interactions.

Figure 2 compares the observed growth with the calculation of the probabilities of finding one and two perturbers closer to the cesium atom than 30 Å, a distance chosen to fit the probability curve to the observation.¹⁸ The close agreement in this comparison, and with the similar result for a square well,⁵ identifies the first and second satellites as one-perturber and two-perturber interactions.

The appearance of multiple-perturber satellites with evenly spaced frequencies proves that the interactions responsible for satellite formation are additive. Interestingly, this applies equally to the ²P_{1/2} and ²P_{3/2} states. These results thus support the often-used assumption of additivity for calculations of the broadening of neutral-atom spec-

tral lines by atomic collisions.

We acknowledge helpful discussions with W. E. Baylis.

-
- ¹W. R. Hindmarsh and J. M. Farr, *Prog. Quantum Electron.* **2**, 141 (1972).
²R. E. M. Hedges, D. L. Drummond, and A. Gallagher, *Phys. Rev. A* **6**, 1519 (1972).
³J. F. Kielkopf, *J. Phys. B* **11**, 25 (1978).
⁴W. R. Hindmarsh and J. M. Farr, *J. Phys. B* **2**, 1388 (1969).
⁵N. F. Allard, *J. Phys. B* **11**, 1383 (1978).
⁶W. E. Baylis, *J. Phys. B* **10**, L477 (1977).
⁷W. E. Baylis, unpublished.
⁸D. G. McCartan and W. R. Hindmarsh, *J. Phys. B* **2**, 1396 (1969).
⁹J. Lorenzen and K. Niemax, *Z. Naturforsch.* **32a**, 853 (1977).
¹⁰R. J. Exton and W. L. Snow, *J. Quant. Spectrosc. Radiat. Transfer* **20**, 1 (1978).
¹¹T. Yabuzaki, A. C. Tam, S. M. Curry, and W. Harper, *Phys. Rev. Lett.* **41**, 543 (1978).
¹²J. F. Kielkopf, *J. Opt. Soc. Am.* **68**, 1447 (1978).
¹³N. F. Allard, S. Sahal-Brechot, and Y. G. Biraud, *J. Phys. B* **7**, 2158 (1974).
¹⁴J. F. Kielkopf, *J. Phys. B* **9**, 1601 (1976).
¹⁵The methods are discussed in Ref. 3 and will be elaborated in a future article.
¹⁶J. Pascale and J. Vandeplanque, *J. Chem. Phys.* **60**, 2278 (1974).
¹⁷W. E. Baylis, *Phys. Rev. A* **1**, 990 (1970).
¹⁸S. Chandrasekhar, *Rev. Mod. Phys.* **15**, 1 (1943).

Propagating Thermal Modes in a Fluid under Thermal Constraint

J. P. Boon

Faculté des Sciences C.P. 231, Université Libre de Bruxelles, 1050 Bruxelles, Belgium

and

C. Allain and P. Lallemand

Laboratoire de Spectroscopie Hertzienne, Ecole Normale Supérieure, 75231 Paris Cedex 05, France

(Received 9 April 1979)

In a stably stratified fluid layer there is a transition beyond which an oscillatory behavior appears. Using forced-Rayleigh-scattering spectroscopy, we found experimental evidence for the existence of propagating modes in agreement with the theoretical predictions.

The Rayleigh-Bénard problem¹ has been the subject of a considerable resurgence of interest in recent years both theoretically² and experimentally.^{3,4} Most of the experimental work has

been devoted to the study of the convection regime and more recently to higher-order transitions leading eventually to turbulence.⁵ The subcritical region has also been investigated theoretical-

ly^{6,7} and experimentally.^{8,9} In particular, critical slowing down was observed for the thermal diffusivity mode as a result of coupling with the vorticity mode. This is illustrated in Fig. 1 for the region $0 \leq R \leq R_c$, where R is the Rayleigh number and R_c its critical value above which convection sets in. We now examine the situation for negative values of R ; that is when the fluid layer (with positive thermal expansion coefficient) is heated from above. Then the external force exerted on the system has a stabilizing effect and no instability is expected.

For the sake of simplicity, let us consider the case of free boundary conditions. The dispersion equation obtained from the hydrodynamic matrix analysis⁷ has the solution

$$\lambda_{\pm} / (\nu\kappa)^{1/2} k^2 = \frac{1}{2}(\sigma^{1/2} + \sigma^{-1/2}) \pm \left[\frac{1}{4}(\sigma^{1/2} - \sigma^{-1/2})^2 + R/R_c(a) \right]^{1/2}. \quad (1)$$

Equation (1) expresses the relaxation rates for the two coupled modes with wave number k ; $\sigma = \nu/\kappa$ is the Prandtl number with ν the kinematic viscosity and κ the thermal diffusivity; $R_c(a)$ is the critical Rayleigh number whose value is determined by the horizontal component a of the fluctuation wave vector k (using reduced units we take $a = 2\pi dl^{-1}$ with d the thickness of the fluid layer and l the horizontal wavelength of the fluctuation). At $R = 0$, one finds the usual (decoupled) modes: $\lambda_-^0 = \kappa k^2$ and $\lambda_+^0 = \nu k^2$. So for a fluid with Prandtl number larger than 1 (e.g., water, ethanol, ...) λ_- is the slow mode which decreases towards zero when R approaches $R_c(a)$ (critical slowing down) whereas the other mode increases to the value $\lambda_+^c = (\nu + \kappa)k^2$ (see Fig. 1).

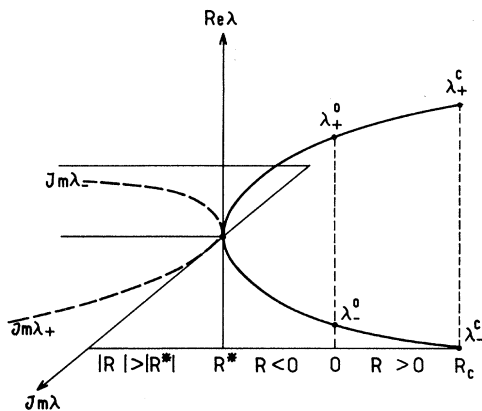


FIG. 1. Representation of the behavior of the modes λ_+ and λ_- .

When the fluid layer is heated from above, R becomes negative and there is a characteristic value of the temperature gradient for which the discriminant in (1) vanishes: $R^* = -R_c(a)(\sigma - 1)^2/4\sigma$. At $R = R^*$, the two modes are degenerate: $\lambda_{\pm} = \frac{1}{2}(\nu + \kappa)k^2$ (see Fig. 1), and from this point on, they are no longer distinguishable; let us call it the thermal mode. When the upward directed temperature gradient increases [$|R| > |R^*(a)|$] the dispersion equation exhibits two complex conjugate roots (see Fig. 1):

$$\lambda_{\pm} = \frac{1}{2}(\nu + \kappa)k^2 \pm i\epsilon(a)^{1/2}(\nu\kappa)^{1/2}k^2; \quad \epsilon(a) = [|R| - |R^*(a)|] |R^*(a)|^{-1}. \quad (2)$$

So when the temperature gradient exceeds a characteristic value corresponding to $|R| = |R^*|$, the thermal mode becomes propagating.¹⁰

In contradistinction to the usual Rayleigh-Bénard problem ($R > 0$), when the fluid is heated from above ($R < 0$), the system is overstabilized. Yet there is but a finite amount of heat that can be transported by thermal conduction, and beyond the value R^* , the heat propagates through the layer as a thermal wave with a damping time constant equal to $2(\nu + \kappa)^{-1}k^{-2}$ and a propagation velocity given by $\pm(\nu\kappa)^{1/2}k\epsilon(a)^{1/2}$ (compare to the power law for the convective velocity⁴). Thus the larger the temperature gradient, the larger the velocity and the more pronounced the oscillatory behavior of the thermal mode.

The analysis presented above can be extended to the more realistic case of a fluid layer con-

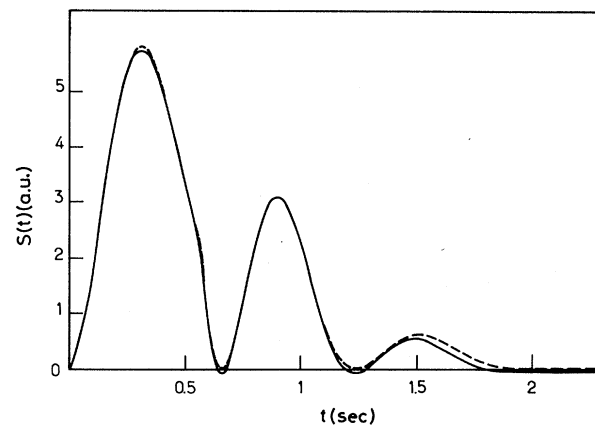


FIG. 2. Typical spectrum as obtained from an experiment performed with acetone at $|R| \approx 69\,000$. The solid line is experimental and the best fit from Eqs. (3) and (4) is represented by the dashed line. The experimental conditions were $d = 0.29$ cm, $l = 0.3$ cm, $\kappa = 1.1 \times 10^{-3}$ cm² sec⁻¹, and $\sigma = 3.6$.

finned between two rigid and perfectly conducting plates.¹¹ We then find that the same theoretical predictions as those obtained for a system with free boundaries hold to a very good approximation provided the kinematic viscosity is changed into an *effective* viscosity $\nu' = \nu f(a)$. $f(a)$ is a numerical factor whose value is given elsewhere⁸ for the first even mode with wave number $k = (a^2 + \pi^2)^{1/2}d^{-1}$.

We have performed an experimental study of the problem described above by using forced-Rayleigh-scattering spectroscopy. This method is well adapted to the investigation of propagating thermal modes. Indeed, the heat pulse that impinges on the scattering medium can be prepared so as to exhibit a well-defined geometric temperature pattern along the horizontal direction,

$$E_c(t) \propto e^{-\alpha t} \{ \cos \beta t [\beta e^{\alpha T} \sin \beta T - \alpha(1 - e^{\alpha T} \cos \beta T)] + \sin \beta t [\alpha e^{\alpha T} \sin \beta T + \beta(1 - e^{\alpha T} \cos \beta T)] \} \quad (4)$$

during cooling. The signal actually detected is proportional to $S(t) = |\delta + E(t)|^2$, where δ represents the amount of coherent stray light acting as a local oscillator for heterodyne detection. $S(t)$ has its first maximum at $t_m = 2\pi\beta^{-1}$ which provides a convenient measure of β .

Figure 2 shows a typical spectrum as obtained by imposing a temperature gradient corresponding to $|R| \approx 69\,000$. The best fit to the experimental data yields the values $\alpha = 1.76 \text{ sec}^{-1}$ and $\beta = 5.14 \text{ sec}^{-1}$ (with an uncertainty of the order of 10%)

which also sets the wavelength of the mode to be detected. A description of the experimental setup is given elsewhere.⁸ The experiments were carried out with acetone as the active medium with the addition of about 0.5% of aniline in order to provide sufficient absorption at the wavelength of the argon-ion-laser light used for pulsing heat into the fluid. Since thermal waves usually have a large damping coefficient, it is convenient to use heat pulses of long duration. Let us rewrite (2) as $\lambda_{\pm} = \alpha \pm i\beta$ and denote the heat pulse duration by T . We then find that, when a standing wave pattern is excited in the medium, the scattered field to be detected is given by

$$E_H(t) \propto [\alpha + e^{-\alpha t}(\beta \sin \beta t - \alpha \cos \beta t)] \quad (3)$$

during heating;

which are in reasonable agreement with the values predicted by the theoretical model: $\alpha = 1.67 \text{ sec}^{-1}$ and $\beta = 5.61 \text{ sec}^{-1}$.¹² Successive experiments were performed at different values of the temperature gradient. The corresponding values of β obtained from the measure of the t_m 's are plotted as β^2 vs $|R|$ in Fig. 3. The power law $(\text{Im } \lambda_{\pm})^2 \propto |R|$ predicted from Eq. (2) is qualitatively verified. The quantitative discrepancy between the experimental results and the theoretical predic-

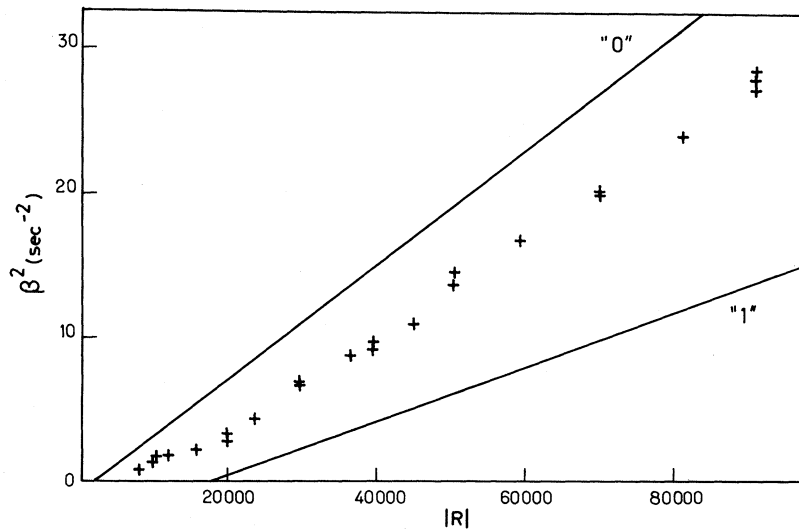


FIG. 3. The squared frequency of the thermal mode as a function of the Rayleigh number. The crosses are the experimental data and the solid lines represent the theoretical predictions for the first even (marked "0") and first odd (marked "1") modes ($d = 0.29 \text{ cm}$, $l = 0.4 \text{ cm}$).

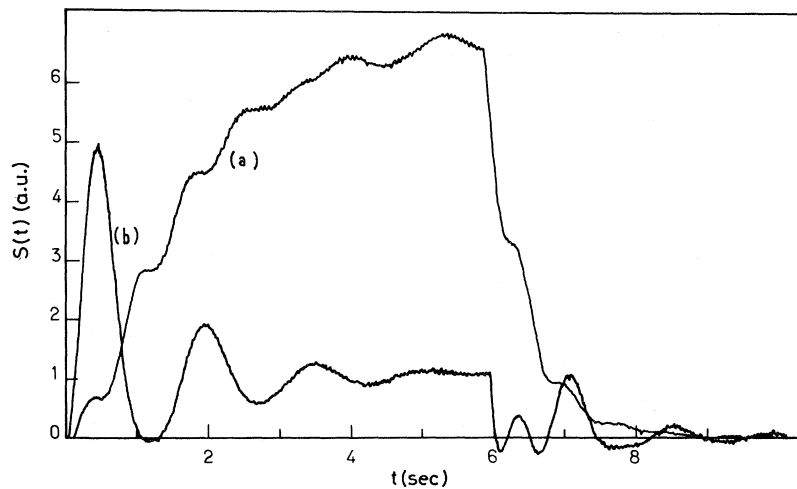


FIG. 4. Example of spectra obtained when exciting the system with a moving heat grating (upper curve, *a*) and with a standing one (lower curve, *b*). The low-amplitude oscillations in the upper spectrum are due to small admixture of heterodyne detection which also manifests itself as undershoots in the cooling region of the lower spectrum ($d=0.53$ cm, $l=0.4$ cm, $|R|=4\times 10^5$).

tions can be interpreted as follows. Because of the presence of a temperature gradient in the scattering cell, the liquid plays the role of an optical prism which induces a bending of the laser beams. As a result, there is nonuniform heating in the vertical plane and therefore both the first even and first odd modes are simultaneously excited, with unknown relative efficiencies. Furthermore, diffraction effects affect the detection beam and it becomes impossible to distinguish the two modes from each other. So the detected signal is a mixture of two signals and the measured value of t_m is intermediate between those corresponding to each mode.¹³

Finally, in order to clearly establish the propagative nature of the thermal wave, we have made use of a moving heat grating to excite the system (see Fig. 2 of Ref. 8). When one moves the grid with the proper speed, the signal detected increases like $[1 - \exp(-\alpha t)]^2$ during a long-duration heat pulse. An illustration is given in Fig. 4 where for comparison the signal obtained from a standing-wave pattern is also shown.

In conclusion, we have presented an analysis of propagating thermal modes in a liquid layer subject to a stabilizing temperature gradient. Using forced-Rayleigh-scattering spectroscopy, we have found experimental evidence for the existence of such modes. Improvement of the accuracy of the experimental results could be achieved by using more elaborate optical techniques to monitor the temperature grating ex-

cited in the fluid,¹⁴ which in turn would require considerable and time-consuming technical sophistication of the instrumentation.

We thank Dr. Paul A. Fleury for stimulating discussions.

¹S. Chandrasekhar, *Hydrodynamic and Hydromagnetic Stability* (Clarendon, Oxford, 1961), Chap. 2.

²C. Normand, Y. Pomeau, and M. G. Velarde, *Rev. Mod. Phys.* **49**, 581 (1977), and references therein.

³E. L. Koschmieder, in *Advances in Chemical Physics*, edited by I. Prigogine and S. A. Rice (Wiley, New York, 1974), Vol. 26, p. 177.

⁴P. Berge, in *Fluctuations, Instabilities and Phase Transitions*, edited by T. Riste (Plenum, New York, 1975), p. 353; G. Ahlers, *ibid.*, p. 181.

⁵G. Ahlers and R. Behringer, *Phys. Rev. Lett.* **40**, 712 (1978); A. Libchaber and J. Maurer, *J. Phys. (Paris), Lett.* **39**, L369 (1978).

⁶V. M. Zaitsev and M. I. Shliomis, *Zh. Eksp. Teor. Fiz.* **59**, 1583 (1971) [*Sov. Phys. JETP* **32**, 866 (1971)].

⁷H. N. W. Lekkerkerker and J. P. Boon, *Phys. Rev. A* **10**, 1355 (1974).

⁸C. Allain, H. Z. Cummins, and P. Lallemand, *J. Phys. (Paris), Lett.* **39**, L473 (1978).

⁹J. Weisfreid, P. Berge, and M. Dubois, *Phys. Rev. A* **19**, 1231 (1979).

¹⁰This is somewhat reminiscent of second-sound propagation in liquid helium. However, care should be taken in making such an analogy which will be analyzed in a more detailed forthcoming paper.

¹¹After this work was completed, our attention was

drawn to the book by G. Z. Gershuni and E. M. Zhukhovitskii, *Convective Stability of Incompressible Fluids* (Keter Publishing House, Jerusalem, 1976); we found that in Sects. 3, 5, and 6 of this monograph, the authors discuss the theoretical aspects of the same problem as analyzed in our present work.

¹²Note that the corresponding Brunt-Väisälä frequency, for purely gravitational waves, defined as $N = (-\nu\kappa R d^{-4})^{1/2}$ (see Ref. 2), would then have the value 6.61 sec^{-1} .

¹³Without a considerably more sophisticated detection

design, it is impossible to predict reliably the relative weight of the two signals. Note that the same cause may be the origin of similar problems in some earlier work (see Ref. 8).

¹⁴The Fourier analysis along the horizontal direction (\sim wavelength l) could also be replaced by a real-space analysis. This method was used in the case of unstable stratification to study the response of the system to a local temperature excitation [B. M. Berkovsky *et al.*, *J. Fluid Mech.* **89**, 173 (1978)] and could be applied to the present problem.

Stochastic Heating of a Large-Amplitude Standing Wave

J. Y. Hsu, K. Matsuda, M. S. Chu, and T. H. Jensen

General Atomic Company, San Diego, California 92138

(Received 20 November 1978)

Stochastic behavior of particle motions in an electrostatic standing wave is analyzed; its significance in supplementary heating of plasmas is discussed.

In heating plasmas with high-power rf waves, a symmetrical structure^{1,2} is often used, which leads to large-amplitude standing waves in the plasma. As a result, stochastic heating of low-energy particles can readily occur. If this stochastic heating happens at the surface of a tokamak where energy is poorly confined, a significant fraction of the rf energy may be lost. The onset of stochasticity may be visualized by drawing phase-space contours of constant particle energies in the presence of each of the two oppositely directed traveling waves alone. If the wave amplitude is sufficiently large, the overlapping of contours allows particles to execute random walks in these two waves. Therefore, the constant of the motion disappears and the trajectory appears to be chaotic.

Applications of stochastic acceleration³ have been studied by Smith and Kaufman⁴ for an obliquely propagating wave and by Kearney and Bers⁵ for a perpendicularly propagating wave. Here, we consider particle motions along the magnetic field lines, or in an unmagnetized plasma in the presence of a standing electrostatic wave, and discuss the stochasticity boundary, the scaling laws of heating, and the modification of the plasma dielectric function due to stochastic electron motion.

We begin our analysis by writing the equation of motion for a particle in a standing wave of fre-

quency ω_0 and wavelength $\lambda_0 = 2\pi/k_0$:

$$d^2X/dT^2 = p \sin X \sin T, \quad (1)$$

where in dimensionless units, $p = eE_0k_0/m\omega_0^2$ is the electric field strength, and $X = k_0x$, $T = \omega_0t$ are the spatial and temporal coordinates. The onset of stochasticity may be found by the criterion of overlapping resonances.³ Decomposing the standing wave into two traveling waves and considering the particle orbits in each of the traveling waves, one finds the particle trapping regions overlap when $p = 1$. This gives a stochasticity boundary at $p \sim 1$. The physical origin of the stochasticity may be illustrated from the spectrum $X_\omega = (1/2\pi) \int_{-\infty}^{+\infty} X(T) e^{i\omega T} dT$. To study the character of the spectrum, we linearize Eq. (1) around the fixed points $X_0^n = n\pi$ (n is an integer) to give

$$d^2X/dT^2 = pX \sin T, \quad (2)$$

where $(-1)^n$ is absorbed into $\sin T$. Equation (2) is a special case of Mathieu's equation, $d^2\psi/d\phi^2 = (b - h^2 \cos^2\phi)\psi$, with the relation $b = h^2/2 = 4p$. It is a general property of Mathieu's equation to exhibit alternating regions of bounded and unbounded solutions in (b, h) space. When $p > p_c = 0.456$, the solution is unbounded.⁶ To understand this "stochastic" instability, Eq. (2) is solved by Fourier